pp. 60–77.
21. T. D. Pollard, *J. Cell Biol.* **91**, 156s (1981); G. A. B. Shelton, Ed., *Electrical Conduction and Behavior in "Simple" Invertebrates* (Clarendon, Oxford, 1982); Y. Fukui and S. Yumura, *Cell Motil. Cytoskeleton* **6**, 662 (1986); H. D. Gortz, Ed., *Paramecium* (Springer-Verlag, New York, 1987).
22. A. G. Kluge, *Chordate Structure and Function* (Macmillan, New York, ed. 2, 1977); J. G. Maisey, *Cladistics* **2**, 201 (1986); H. B. Whittington, *The Burgess Shale* (Yale Univ. Press, New Haven, 1985).
23. L. H. Hyman, *The Invertebrates: Echinodermata* (McGraw-Hill, New York, 1955), vol. 4; A. B. Smith, *Palaeontology* **27**, 431 (1984); S. Smiley, in *Echinoderm Phylogeny and Evolutionary Biology*, C. R. C. Paul and A. B. Smith, Eds. (Oxford Univ. Press, Oxford, in press); R. A. Raff *et al.*, *ibid.*
24. T. H. Huxley, *Q. J. Microsc. Sci.* **15** (1875); K. Grobben, *Verh. Zool. Bot. Ges. Wein* **58**, 491 (1908); S. F. Gilbert, *Developmental Biology* (Sinauer, Sunderland, MA, 1985).
25. R. P. S. Jefferies, *Symp. Zool. Soc. London* **36**, 253 (1975); in (*2*), pp. 443–477.
26. H. B. Whittington, in (*2*), pp. 253–268.
27. A. Naef, *Ergeb. Fortschr. Zool.* **6**, 27 (1924).
28. K. G. Wingstrand, *Galathea Rep.* **16**, 7 (1985).
29. P. P. Iwanoff, *Z. Morphol. Oekol. Tiere* **10**, 62 (1928).
30. J. Vagrolgyi, *Syst. Zool.* **16**, 153 (1967); L. v. Salvini-Plawen, *ibid.* **17**, 192 (1968); C. R. Stasek, in *Chemical Zoology*, M. Florkin and B. T. Scheer, Eds. (Academic Press, New York, 1972), pp. 1–44.
31. L. H. Hyman, *The Invertebrates: Smaller Coelomate Groups* (McGraw-Hill, New York, 1959), vol. 5.
32. R. L. Zimmer, in *Living and Fossil Bryozoa*, G. P. Larwood, Ed. (Academic Press, New York, 1973), pp. 593–599.
33. M. Jones, *Bull. Biol. Soc. Wash.* **6**, 117 (1985).
34. J. T. Bonner, *The Evolution of Development* (Cambridge Univ. Press, Cambridge, 1956).
35. B. Runnegar, *J. Geol. Soc. Aust.* **29**, 395 (1982).
36. G. Vidal, *Sci. Am.* **250**, 48 (February 1984); P. Cloud, *Paleobiology* **2**, 351 (1976); H. J. Hofmann and J. Chen, *Can. J. Earth Sci.* **18**, 443 (1981); J. W. Schopf and D. Z. Oehler, *Science* **193**, 47 (1976); J. W. Schopf, *Sci. Am.* **239**, 110 (September 1978); M. R. Walter, J. H. Oehler, D. Z. Oehler, *J. Paleontol.* **50**, 872 (1976).
37. M. F. Glaesner, *The Dawn of Animal Life* (Cambridge Univ. Press, Cambridge, 1984); R. A. Raff and E. C. Raff, *Nature (London)* **228**, 1003 (1970); B. Runnegar, *Alcheringa* **6**, 223 (1982); A. Seilacher, in *Patterns of Change in Earth Evolution*, H. D. Holland and A. F. Trendall, Eds. (Springer-Verlag, Berlin, 1984), pp. 159–168.
38. M. D. Brasier, in (*2*), pp. 103–159.
39. R. E. Dickerson, *J. Mol. Evol.* **1**, 26 (1971); B. Runnegar, *Palaeontology* **29**, 1 (1985); *Lethaia* **15**, 199 (1982); *J. Mol. Evol.* **22**, 141 (1985).
40. R. J. Britten, *Science* **231**, 1393 (1986); M. Goodman, M. L. Weiss, J. Czelusniak, *Syst. Zool.* **31**, 376 (1982); W.-H. Li and M. Tanimura, *Nature (London)* **326**, 93 (1987).
41. T. Ohama, H. Hori, S. Osawa, *Nucleic Acids Res.* **11**, 5181 (1983).
42. A. Sedgwick, *Q. J. Microsc. Sci.* **24**, 43 (1884).
43. R. Siewing, *Zool. Jahrb. Abt. Anat. Ontog. Tiere* **103**, 439 (1980).
44. L. v. Salvini-Plawen, *Zool. Scr.* **11**, 77 (1982).
45. G. J. Olsen, *Cold Spring Harbor Symp. Quant. Biol.*, in press.
46. R. M. Torczynski, M. Fuke, A. P. Bollon, *DNA* **4**, 283 (1985).
47. L. Nelles, B.-L. Fang, G. Volckhaert, A. Vandenberghe, R. De Wachter, *Nucleic Acids Res.* **12**, 8749 (1984).
48. P. M. Rubtsov *et al.*, *ibid.* **8**, 5779 (1980).
49. J. Messing, J. Carlson, G. Hagen, I. Rubenstein, A. Oleson, *DNA* **3**, 31 (1984).
50. R. McCarroll, G. J. Olsen, Y. D. Stahl, C. R. Woese, M. L. Sogin, *Biochemistry* **22**, 5858 (1983).
51. M. Salim and B. E. H. Maden, *Nature (London)* **291**, 205 (1981).
52. Voucher specimens, where available, have been deposited at California Academy of Sciences, Golden Gate Park, San Francisco, CA. Copies of the sequences and alignments are available on written request. We acknowledge gifts of RNA or animals from R. Anderson, W. Jeffery, J. Ruderman, L. Slobodkin, and J. Valois. We thank B. Parr and J. M. Turbeville for comments on the manuscript. Supported by NSF grants BSR 85-16582 (R.A.R., N.R.P., M.T.G., and E.C.R.) and DCB 83-02149 (E.C.R.); NIH grants GM34527 (N.R.P.), HD21337 (R.A.R.), and HD16739 (E.C.R.); Office of Naval Research grant N14-86-K-0268 (G.J.O. and N.R.P.); and a MacArthur Prize Fellowship (M.T.G.).

Research Articles

Glycosyl-Phosphatidylinositol Moiety That Anchors *Trypanosoma brucei* Variant Surface Glycoprotein to the Membrane

MICHAEL A. J. FERGUSON, STEVE W. HOMANS, RAYMOND A. DWEK, THOMAS W. RADEMACHER

Two forms of protein-membrane anchor have been described for the externally disposed glycoproteins of eukaryotic plasma membranes; namely, the hydrophobic transmembrane polypeptide and the complex glycosylphosphatidylinositol (G-PI) moiety. The chemical structures of the major species of G-PI anchors found on a single variant surface glycoprotein (VSG) of the parasitic protozoan *Trypanosoma brucei* were determined by a combination of nuclear magnetic resonance spectroscopy, mass spectrometry, chemical modification, and exoglycosidase digestions. The G-PI anchor was found to be heterogeneous with respect to monosaccharide sequence, and several novel glycosidic linkages were present. The results are pertinent to the mechanism of the biosynthesis of G-PI anchors.

THE PARASITIC PROTOZOAN *Trypanosoma brucei* HAS A CONtinuous cell-surface coat made up of a tightly packed monolayer of variant surface glycoprotein (VSG) molecules. This VSG coat acts as a macromolecular diffusion barrier protecting the parasite from lytic host-serum components. A single trypanosome expresses only one type of VSG (variant) at a time, but has several hundred VSG genes encoding immunologically distinct VSG variants. It is the sequential expression of different VSG coats that allows the parasite to evade the host's immune response by antigenic variation (*1*). All of the different VSG variants analyzed have molecular sizes of about 55 kD and one or more asparagine glycosylation sites. Despite the lack of extensive primary amino acid sequence homology the VSG molecules are thought to share similar tertiary structures (*2*).

The authors are members of the Oxford Oligosaccharide Group, Department of Biochemistry, University of Oxford, South Parks Road, Oxford, OX1 3QU, England.

From the comparison of complementary DNA (cDNA) sequences and VSG carboxyl-terminal peptide sequences (*1*) and from biosynthetic studies (*3*) it appears that VSG messenger RNA (mRNA) encodes a short COOH-terminal hydrophobic domain which is rapidly removed after polypeptide synthesis (<1 minute) and directly replaced by the addition of a glycosyl-phosphatidylinositol (G-PI) moiety. The G-PI moiety serves as the sole anchor to the membrane for the glycoprotein which then traverses the Golgi stacks to the plasma membrane. The membrane binding form of the glycoprotein (mfVSG) can be converted to a water soluble form (sVSG) by the action of an endogenous G-PI–specific phospholipase C (GPI-PLC) which removes the hydrophobic diacylglycerol group from the G-PI anchor (*4*).

The VSG G-PI anchor includes an amide linkage from the COOH-terminal amino acid α-carboxyl group to an ethanolamine residue, which bridges the VSG polypeptide to a mannose- and galactose-containing glycan (*5*). In addition, the glycan is known to contain a glucosamine residue (*6*) that is not *N*-acetylated and that is glycosidically linked to dimyristylphosphatidylinositol (*7*). We now report the complete chemical structure of the G-PI moiety present on a *T. brucei* variant surface glycoprotein.

Preparation of VSG and G-PI components. Trypanosome clones, MITat 1.4 (variant 117), of *T. brucei* strain 427 were purified from infected rat blood (*8*). Trypanosomes were also cultured in vitro with [9,10-^{3}H]myristic acid (*9*) for 1 hour before processing to produce biosynthetically labeled mfVSG. The isolation of the glycan moieties (NG) from mfVSG is described in Fig. 1. The mfVSG and sVSG glycoproteins were purified (*8*, *10*), and the intact G-PI moiety was prepared by Pronase digestion of mfVSG (*11*) and purified by HPLC (high-performance liquid chromatography) (*12*). Demyristylated G-PI (dMG-PI) was prepared from G-PI by the action of a mild base (*13*), and *N*-acetylated dMG-PI (NAc-dMG-PI) was prepared as described (*14*). The sVSG COOH-terminal glycopeptide (sCt-gp) represents the entire G-PI anchor attached to the COOH-terminal aspartic acid residue minus the dimyristylglycerol lipid moiety and was purified as described earlier (*11*).

Chemical analysis. Purified sCt-gp (800 nmol) was analyzed by one- and two-dimensional ^{1}H NMR (nuclear magnetic resonance) (Fig. 2A) and by GC-MS (gas chromatography–mass spectrometry) analysis (Tables 1 and 2). Unfractioned NG was analyzed by GC-MS compositional analysis (Table 1) and GC-MS methylation analysis before and after digestion with coffee bean α-galactosidase (Table 2). Gel-filtration on Bio-Gel P-4 (Fig. 3) resolved NG into three fractions (NG1, NG2, and NG3), which were subsequently analyzed by one-dimensional ^{1}H NMR (Fig. 2B) and GC-MS for composition (Table 1). The NG1, -2, and -3 fractions were also permethylated, purified by reversed-phase HPLC (*15*), and subjected to methylation analysis (Table 2). A sample of ^{3}H-labeled NG was also analyzed by Bio-Gel P-4 chromatography in order to determine the precise relative hydrodynamic volumes of the various neutral glycan species (Table 3).

Methylation analysis showed that all NG fractions contain three mannose residues per mole (one nonreducing terminal mannose, one 2-*O*–substituted mannose, and one 3,6-di-*O*–substituted mannose) (Table 2). Galactose residues are attached to the 3-position of the 3,6-di-*O*–substituted mannose residue since digestion with coffee bean α-galactosidase yields a single glycan species (Table 3) in which the 3,6-di-*O*–substituted mannose is quantitatively replaced by a 6-*O*–substituted mannose residue (Table 2). Treatment of unfractionated NG with a mixture of coffee bean α-galactosidase and jack bean α-mannosidase produced one major product at 1.7 glucose units as shown by Bio-Gel P-4 chromatography, which corresponds to free 2,5-anhydromannitol (2,5-AHM) (Table 3). Purified NG1, -2, and -3, isolated by Bio-Gel P-4 chromatography, were individually treated with the Manα1-2Man–specific α-mannosidase from *Aspergillus phoenicis* (*16*). In all cases further analysis on Bio-Gel P-4 showed a reduction in hydrodynamic volume of approximately one glucose unit, consistent with the removal of one terminal α1-2–linked mannose residue common to all or most of the structures (Table 3). These data, together with interresidue nuclear

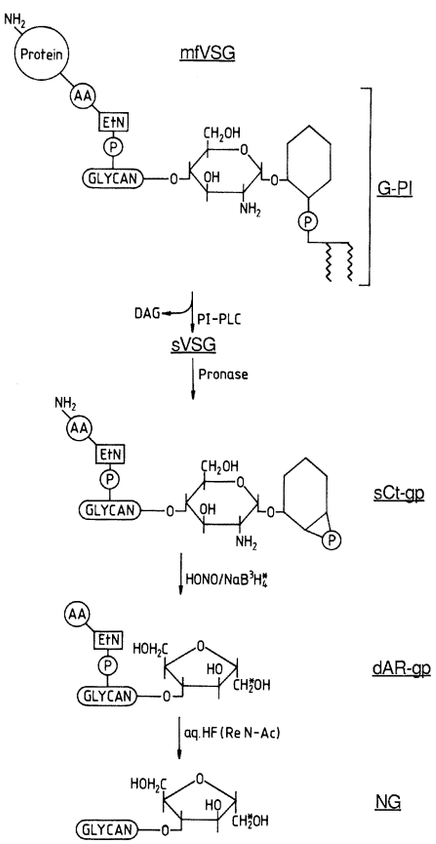

Fig. 1. Isolation of G-PI glycan fragments for structural analysis. In this study mfVSG was converted to sVSG by the action of the endogenous trypanosome GPI-PLC, which removes the diacylglycerol (DAG) moeity. Exogenous bacterial phosphatidylinositol specific phospholipase C (PI-PLC) may be used instead (*7*). The sVSG COOH-terminal glycopeptide (sCt-gp) was produced by Pronase digestion and purified (*11*). The sCt-gp (800 nmol) was dissolved in 200 μl of 0.1*M* sodium acetate, *p*H 4.0, and deaminated (200 μl of 0.5 $NaNO_2$; 2.5 hours); the material was then split into two portions of 760 and 40 nmole and reduced with $NaBH_4$ and NaB^3H_4, respectively; reduction was achieved by adding 0.26 volume of 400 m*M* boric acid, 1.26*M* NaOH, followed immediately by 1.26 volumes of either 1*M* $NaBH_4$ or 12 m*M* NaB^3H_4 (8 Ci/mmol) in 50 m*M* NaOH, boric acid buffer *p*H 11.0. Reduction was continued for 3 hours in both cases, except that excess $NaBH_4$ was added to the NaB^3H_4-treated sample after the first 80 minutes. The reduced oligosaccharitols with 2,5-anhydromannitol termini were desalted after acidification by passage through AG50X12(H^+) and methanol evaporation. Material reduced with NaB^3H_4 had radiochemical impurities removed by descending chromatography on Whatman 3 MM paper for 60 hours in 1-butanol, ethanol, water system (4:1:1). The labeled oligosaccharitols remained at the origin and were eluted with water. They were further purified by high-voltage electrophoresis on Whatman 3 MM paper for 30 minutes at 80 V/cm in pyridine, acetic acid, and water (3:1:387), *p*H 5.4. The acidic oligosaccharitols (a broad series of overlapping peaks) were eluted from the paper with water, passed through 0.1 ml of Chelex 100(Na^+) over 0.2 ml of AG50X12(H^+) and filtered through a 0.5-μm Teflon membrane. The specific activity of the deaminated and reduced glycopeptide (dAR-gp) was 1 Ci/mmol; half of this material (20 μCi) was added to the bulk $NaBH_4$ reduced material to act as labeled tracer. The dAR-gp fraction was dephosphorylated with 50 μl of 50 percent aqueous HF at 0°C for 38 hours. The sample was added to 275 μl of frozen saturated LiOH. The LiF precipitate was removed by centrifugation and washed twice with 50 μl of H_2O. The pooled supernatants were neutralized with 100 μl of saturated $NaHCO_3$; the salt was removed on a column of 0.2 ml of Chelex 100(Na^+) layered over 1 ml of AG50X12(H^+), over 0.8 ml of AG3X4(OH^-), over 0.2 ml of QAE-Sephadex A25 equilibrated with water. After filtration through a 0.5-μm Teflon filter the final yield of the neutral glycan (NG) fraction was about 70 percent. For other G-PI anchors containing *N*-acetylhexosamines a second *N*-acetylation step (RE N-Ac) is necessary. Abbreviations: AA, the COOH-terminal aspartic acid residue; EtN, ethanolamine; and P, phosphate. The hexagon represents *myo*-inositol.

Overhauser effect (NOE) measurements (Fig. 2) are consistent with the following composite structure:

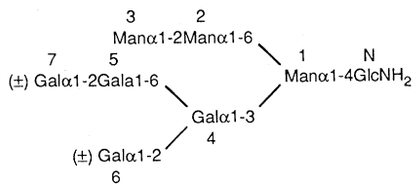

The heterogeneity of the α-galactose antennae branch is evident from the composition and methylation analyses (Tables 1 and 2) and ^{1}H-NMR spectra (Fig. 2) of the sCt-gp and NG fractions. The smallest fraction from Bio-Gel P-4 gel-filtration, NG3 (Fig. 3), contains one terminal nonreducing galactose residue and one 6-*O*–substituted galactose residue, which defines this branch as Galα1-6Galα1-. The methylation analysis of NG2 shows both 2,6-di-*O*–substituted galactose and 2-*O*–substituted galactose present in a ratio of 7:3 (Table 2), indicating the presence of two monosaccharide sequences in this fraction. The NG2 fraction therefore contains an α1-2 linked galactose residue, which can be found linked to either the galactose-5 residue of the NG3 structure forming a linear sequence Galα1-2Galα1-6Galα- or to the internal galactose-4 residue of the NG3 structure forming a second antennae Galα1-2(Galα1-6)Galα-. The NG1 fraction has one more α1-2 linked galactose residue than NG2 and contains the sequence Galα1-2Galα1-6(Galα1-2)-Galα1- (Fig. 2).

The four major glycan structures described account for about 70 percent of the glycans. A further 15 percent can be accounted for in fractions NGA and NGB (Fig. 3) which most likely represent structures containing five or more and one or no galactose residues, respectively (Table 1). Other minor species (15 percent) present in the NG1 and NG2 fractions contain 2,3-di-*O*–substituted mannose (Table 2). These minor species have not been defined further.

The bridge between the G-PI moiety and the COOH-terminal aspartate residue involves an ethanolamine residue in an amide linkage to the aspartyl α-carboxyl group (*5*). Periodate oxidation was used to confirm that the ethanolamine is in a phosphodiester

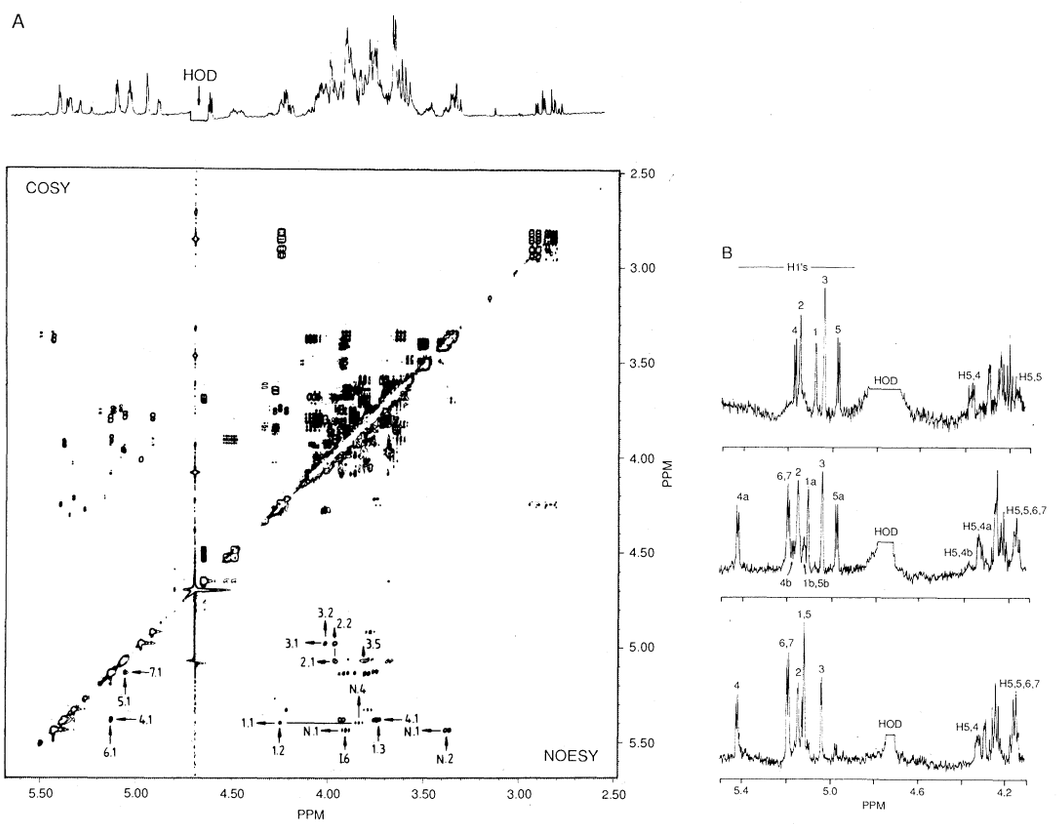

Fig. 2. ^{1}H NMR spectra of the sCt-gp and NG fractions. (**A**). The unfractionated sCt-gp structures were analyzed by high-resolution two-dimensional ^{1}H-^{1}H correlated spectroscopy (COSY), top left of figure. The spectrum was recorded as described (*38*) with a sweep width of ±1300 Hz, and 1024 data points in each dimension. For each t_1 increment 64 transients were collected. Time domain data were apodized in each dimension by means of a phase-shifted (π/12) sine-bell function. Both negative and positive contour levels are plotted with positive intensity. The one-dimensional spectrum obtained upon Fourier transformation of the data at $t_1 = 0$ is shown above. Off diagonal peaks (cross-peaks) correlate protons between which a resolved scalar (J) coupling exists. Through-bond–coupled protons were identified, and most of the resonances in the one-dimensional spectrum could be assigned stepwise from the resolved anomeric (H-1) protons (which resonate in the region 4.9 to 5.5 ppm). The magnitudes of the scalar (J) coupling between the H-1 and H-2 protons (*39*), which were measured from the splitting of the H-1 protons in one-dimensional spectra (B), were used to determine the monosaccharide residue type and the anomeric configuration. The presence of primary sequence heterogeneity in the unfractionated sCt-gp structures was evident in the one-dimensional NMR spectrum by the presence of anomeric proton resonances of less than unit intensity. The additional spectral dispersion afforded by the COSY experiment allowed the connectivity networks for each residue to be traced separately, and four major species could be identified. After resonance assignment, all through-space connectivities between proximal protons (<4 Å distant) were mapped by use of ^{1}H-^{1}H nuclear Overhauser effect spectoscopy (NOESY) as described previously (*38*), bottom right of figure. The spectrum was recorded under identical conditions to the COSY experiment with a mixing time of 500 msec. The cross-peaks in NOESY, for this particular mixing time, generate qualitative through-space connectivities within the molecule. Connectivities were assigned to specific protons by means of the resonance assignments derived from COSY. Intraresidue and interresidue through-space connectivities were defined for each structure, and the primary sequences of the monosaccharide residues were determined stepwise along the molecule with the use of these connectivities and methylation analysis data. Representative connectivities are shown for the largest glycan structure, where the cross-peak label abbreviations correspond with the residue descriptors (described in the text) followed by the ring proton number. Cross-peaks labeled I are due to inositol. (**B**) One-dimensional ^{1}H NMR spectra of major neutral glycan fractions NG3 (top panel), NG2 (middle panel), and NG1 (lower panel). Each spectrum was recorded with a sweep width of ±1300 Hz, 16,384 data points, and 200 transients. The chemical shift axis is referenced to acetone, δ = 2.225 ppm at 30°C. The proposed resonance assignments are deduced from the magnitudes of J_{12} (*39*) and from the characteristic chemical shifts observed between fractions, which are due to differences in primary sequence. The notation corresponds with that described earlier. In the middle panel, the a and b for residues 1, 4, and 5 correspond to each of the two structures found in fraction NG2.

linkage to the 6-position of either the terminal or the penultimate 2-*O*–substituted mannose as suggested by the presence of mannose-6-phosphate in the methanolyzates of sCt-gp (Table 1). In either case, periodate oxidation would cleave the mannose residue between C-3 and C-4 to yield a [1-^{2}H]glycerol group after reduction with NaB^2H_4 (derived from mannose C-4, C-5, and C-6), with the phosphorylethanolamine–aspartic acid group remaining attached to the mannose-6-hydroxyl (Fig. 4A). In addition, acid hydrolysis was used on the periodate-oxidized and NaB^2H_4-reduced demyristylated

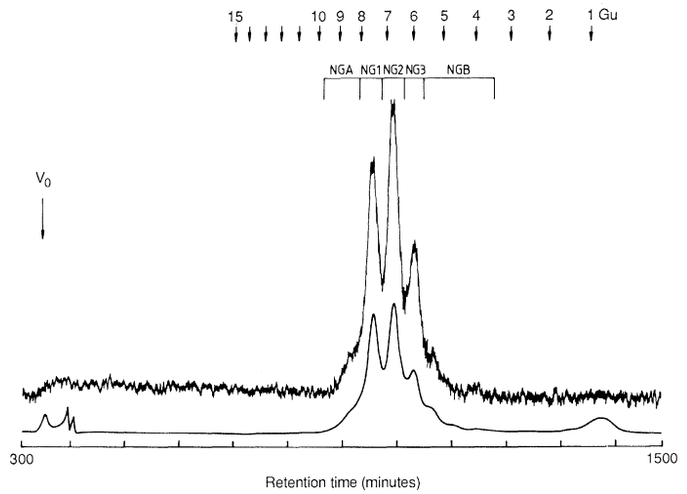

Fig. 3. Bio-Gel P-4 chromatography of the neutral glycan (NG) fraction. The ^{3}H-labeled neutral glycan (NG) fraction of the mfVSG G-PI anchor (Fig. 1) was fractionated on two columns in series (1.5 × 100 cm each) packed with Bio-Gel P-4 (−400 mesh) held at 55°C and eluted with water at 0.2 ml/min. The eluate was monitored for radioactivity (Berthold LB503 radioactivity flow monitor) and refractive index (Erma ERC7510 monitor) before collection in 0.5-ml fractions. The upper broad trace represents radioactivity and the lower smooth trace refractive index. The major peaks NG1, NG2, and NG3 and the minor flanking regions NA and NB were pooled separately for analysis. The numbers at the top represent the elution positions of dextran oligomers (number of glucose units) determined in a separate experiment.

Table 1. Compositional analyses. All analyses were performed in the presence of a *scyllo*-inositol internal standard. Samples were subjected to methanolysis (50 μl of 0.5*M* HCl, 20 percent methyl acetate in dry methanol, 20 hours, 70°C), *N*-acetylation (by the subsequent addition of 10 μl of pyridine and 5 μl of acetic anhydride, 30 minutes at room temperature) and trimethylsilylation (TMS) with 15 μl of Sil-A (Sigma) after drying. The TMS derivatives were analyzed with a Hewlett-Packard 5996 GC-MS equipped with an open-split interface for simultaneous mass spectral identification and flame ionization detector (FID) quantitation. Spectra were recorded by electron-impact (70 eV). A fused silica bonded phase column 25 m × 0.32 mm (RSL150, Alltech) with He as carrier gas at 3 ml/min was used in the GC system. Direct on-column injection was used with a temperature program of 140°C (2 minutes) and a linear gradient to 250°C at 6° per minute, held for 15 minutes. All figures shown here and in Table 2 and Fig. 5 are means of at least two analyses and are subject to experimental error of ±15 percent. ND, not determined.

Material	Proportion (%)*	Molar ratio				
		2,5-AHM	Man	Gal	Man-6-P†	*myo*-inositol
sCt-gp		0.0	2.0	3.7	0.5	0.0‡
dAR-gp		1.0	2.0	4.0	ND	0.0‡
NG	100	1.0	2.8	3.7		0.7
Bio-Gel P-4 fractions§						
NGA	7	0.9	3.0	5.4		
NG1	30	1.0	3.0	3.9		
NG2	40	1.1	3.0	3.0		
NG3	15	0.9	3.0	2.0		
NGB	8	0.6	3.0	1.5		

*Percentage of the total ^{3}H label in each fraction. †Analyses for mannose-6-phosphate were as described above except that after trimethylsilylation the products were dried, redissolved in 10 percent methanol in ether (0°C, 10 minutes) and treated twice with an equal volume of ether saturated with diazomethane at 0°. The dimethyl phosphate derivatives were dried, redissolved in Sil A (Sigma), and analyzed as described, above. ‡Absent in these analyses due to the acid stability of the inositol-phosphate and glucosamine-inositol bonds to methanolysis (*7*). §See legend to Fig. 3.

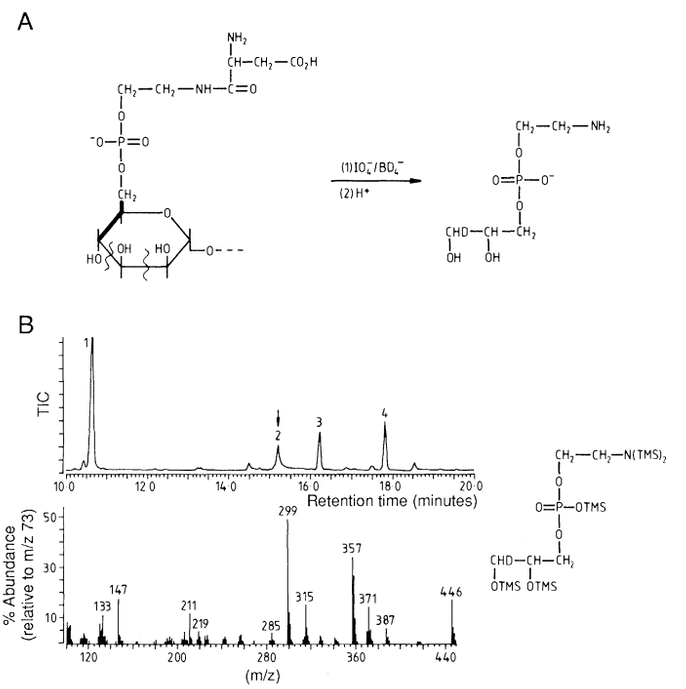

Fig. 4. Periodate oxidation of the mannose-6-phosphorylethanolamine bridge. (**A**) The wavy lines indicate the sites of periodate oxidation cleavage. The bold lines indicate the regions of the mannose carbon backbone which survive oxidation. Periodate oxidation was performed on 120 nmol of dMG-PI in 30 m*M* $NaIO_4$, 200 m*M* sodium acetate buffer, *p*H 4.5, containing 0.1 percent 1-propanol as radical scavenger. Oxidation was performed at twofold molar excess of periodate over theoretical oxidation sites (estimated as 13 mol per mole of dMG-PI) at 4°C in the dark. The reaction was followed by monitoring the decrease in absorbance due to the IO_4^- ion at 223 nm after dilution (1:300) of small portions with water. Oxidation reached a maximum by about 15 hours. After 20 hours, the reaction was stopped by making the solution 1 percent (by volume) with respect to ethylene glycol. After 30 minutes, the products were reduced by the addition of an equal volume of 1*M* NaB^2H_4 in 1*M* NH_4OH (final *p*H 9.8). After 3 hours, the excess NaB^2H_4 was destroyed with acetic acid, and the mixture was desalted by passage through AG50X12(H^+), followed by repeated evaporation with acidified methanol. (**B**) Periodate oxidized and borodeuteride-reduced dMG-PI was hydrolyzed (2*M* HCl, 100°C, 4 hours), dried, and trimethylsilylated with the reagent described in (*40*). The products were analyzed by GC-MS as described in the legend to Table 1 except that the GC program was 100°C (held for 2 minutes) to 260°C at 6° per minute. The total ion chromatogram (upper panel) shows the presence of [1-^{2}H]erythritol-TMS_4 (peak 1) and α- and β-mannose-TMS_5 (peaks 3 and 4). Peak 2 had the same retention time and mass spectrum (lower panel) as the TMS derivative of authentic glycerophosphoryl ethanolamine generated by deacylation of phosphatidylethanolamine (*13*). The spectrum shows the ions characteristic of a [1-^{2}H]glycerophosphoryl derivative at *m/z*.

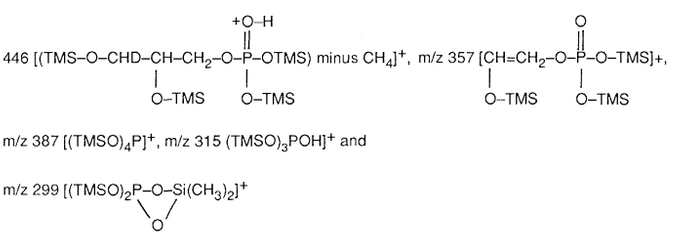

G-PI (dMG-PI) to exploit the relatively acid-stable phosphodiester linkage while quantitatively removing the acid-labile aspartic acid group. After trimethylsilylation of the above, [1-^{2}H]glycerophosphoryl ethanolamine was identified by GC-MS (Fig. 4B) and confirmed the presence of ethanolamine phosphate linked to the 6-position of mannose.

Susceptibility to digestion by jack bean α-mannosidase was used to probe the position of the ethanolamine phosphate bridge. From the substrate specificity of jack bean α-mannosidase the terminal mannose residue should be resistant to digestion only if this residue is the site of the ethanolamine phosphate linkage. The deaminated and reduced glycopeptide (dAR-gp) fraction, which still contains the aspartic acid–ethanolamine phosphate bridge (Fig. 1), was first treated with coffee bean α-galactosidase to remove the α-galactosyl branch heterogeneity. Subsequent cold aqueous hydrogen fluoride dephosphorylation produced one major elution product with 4.2 glucose units on Bio-Gel P-4, corresponding to the Manα1-2Manα1-6Manα1→4,2,5-AHM region (Table 3). Digestion of this neutral structure with jack bean α-mannosidase converted this peak to one at 1.7 glucose units (2,5-anhydromannitol). In contrast, digestion of the agalactosyl dAR-gp with the α-mannosidase prior to HF dephosphorylation and Bio-Gel P-4 analysis failed to remove any of the α-mannose residues. This result suggests that it is the terminal α-mannose residue that is linked to the ethanolamine phosphate bridge.

Periodate oxidation was also used to probe the mannose→glucosamine→inositol monosaccharide sequence. The predicted sites of periodate oxidation of the demyristylated G-PI (dMG-PI) fraction are shown in Fig. 5A; the hexose residues not shown have free hydroxyl groups at C-3 and C-4 and will be oxidized and reduced to [1-^{2}H]glycerol. The periodate-oxidized and NaB^{2}H$_4$-reduced dMG-PI was hydrolyzed, treated with alkaline phosphatase, and analyzed by GC-MS after peracetylation of the products (Fig. 5B). The three predicted major products were found: [1-^{2}H]glycerol, an intact mannose residue (derived from the protected 3,6-di-*O*–substituted mannose branch-point residue), and [1-^{2}H]erythritol (derived from the glucosamine residue) (Fig. 5B).

^{1}H NMR data suggest that the glucosamine is linked α1–6 to the *myo*-inositol residue as evidenced by a NOE linking GlcNH$_2$ H-1 to inositol H-6 (Fig. 2A). The predicted oxidation and reduction product of the inositol ring is therefore [1,4-di-^{2}H]threitol (derived from carbons 1, 2, 5, and 6). However this component was observed only in trace amounts in the products of periodate oxidation of the dMG-PI sample described above. On the basis of the observations of (*17*) it is likely that this product is lost because of the rapid overoxidation of the glucosamine residue from C-2, and onward through to the inositol ring. *N*-Acetylation of the glucosamine residue present on dMG-PI renders the residue resistant to periodate oxidation (Fig. 5A). The NAc-dMG-PI was treated as above for dMG-PI, and Fig. 5C shows the recovery of [1-^{2}H]glycerol, an intact protected mannose residue as before, and intact *N*-acetylglucosamine in place of the [1-^{2}H]erythritol. In addition, the predicted [1,4-di-^{2}H]threitol product is now observed in good yield. A di-deuterated tetritol can only arise from the prior oxidation of a polyol (in this case *myo*-inositol) and not from a hexose or hexosamine, which can only generate a monodeuterated tetritol. From the stereochemical arrangement of the *myo*-inositol ring, threitol must be derived from carbons at positions 1, 2, 5, and 6. This implies that the inositol ring was originally substituted at C-1 and C-6. The phosphatide group is known to be at C-1 (*7*), thus leaving only C-6 for glycosidic substitution by the glucosamine residue.

Table 2. Methylation analyses. In all cases samples were permethylated according to (*35*). Permethylated glycans were hydrolyzed (2.5 hours at 80°C in 100 μl of 0.25*M* H_2SO_4, 93 percent aqueous acetic acid), applied to a 0.5-ml column of AG3X4 (acetate form) and eluted with five column volumes of 50 percent aqueous methanol. Following repeated evaporation with toluene the hydrolyzates were reduced with NaB^{2}H$_4$ (200 μl; 10 mg/ml; 3 hours) with sonication. Excess NaB^{2}H$_4$ was destroyed with acetic acid, and boric acid was removed by repeated evaporation (five times) with 0.2 ml of methanol. The products were dried and acetylated with 250 μl of acetic anhydride (100°C, 2.5 hours). The acetic anhydride was removed at reduced pressure. The resulting partially methylated alditol acetates (PMAA's) were recovered by partitioning between CH_2Cl_2 and water. The CH_2Cl_2 phase was concentrated to about 20 μl, and 2-μl portions were analyzed by GC-MS (Supelcowax 10 column, 30 m by 0.32 mm; Supelco) with He as carrier gas (2.5 ml/min) and direct on-column injection. The temperature program was started at 90°C (1 minute) followed by a linear gradient to 140°C at 30°C per minute, and then to 250°C at 5°C per minute, and held for 15 minutes. The PMAA's were identified by their characteristic mass spectra and retention times, and were quantified by their flame-ionization detector response with semiempirical molar correction factors (*36*).

PMAA	Origin	sCt-gp*	NG	α-Galactosidase treated NG	Subfractions		
					NG1	NG2	NG3
2,5-Anhydro mannitol†							
(1,3,6-tri-*O*-methyl-4-*O*-acetyl)	4-*O*-subs. 2,5-AHM	0.0	†	†	†	†	†
Mannitol							
(2,3,4,6-tetra-*O*-methyl-1,5-di-*O*-acetyl)	Terminal-Man	0.6	1.0	1.0	1.0	1.0	1.0
(3,4,6,-tri-*O*-methyl-1,2,5-tri-*O*-acetyl)	2-*O*-subs. Man	1.0	1.0	1.0	1.2	1.0	1.3
(2,3,4-tri-*O*-methyl-1,5,6-tri-*O*-acetyl)	6-*O*-subs. Man	0.0	0.0	0.9	0	0.0	0.0
(2,4-di-*O*-methyl-1,3,5,6-tetra-*O*-acetyl)	3,6-*O*-disubs. Man	0.9	0.9	0.0	0.9	0.8	1.1
(4,6-di-*O*-methyl-1,2,3,6-tetra-*O*-acetyl)	2,3-*O*-disubs. Man	0.2	0.2	0.0	0.1	0.2	0.0
Galactitol							
(2,3,4,6-tetra-*O*-methyl-1,5-di-*O*-acetyl)	Terminal-Gal	2.0	1.7	[0.8]‡	1.9	1.7	0.9
(2,3,5,6-tetra-*O*-methyl-1,4 di-*O*-acetyl)		0.0	0.0	[0.9]‡	0.0	0.0	0.0
(3,4,6,-tri-*O*-methyl-1,2,5-tri-*O*-acetyl)	2-*O*-subs. Gal	0.3	0.4	0.0	1.0	0.3	0.0
(2,3,4-tri-*O*-methyl-1,5,6-tri-*O*-acetyl)	6-*O*-subs. Gal	0.4	0.4	0.0	0.0	0.3	1.1
(3,4-di-*O*-methyl-1,2,5,6-tetra-*O*-acetyl)	2,6-*O*-disubs. Gal	1.0	0.6	0.0	1.0	0.7	0.0
2-*N*-Methylacetamido-2-deoxyglucitol							
(3,6-di-*O*-methyl-1,4,5-tri-*O*-acetyl)	4-*O*-subs. GlcNAc	0.6*	—	—	—	—	—

*The intact sCt-gp sample (35 nmol) was subjected to methylation analysis following *N*-acetylation in 100 μl of saturated $NaHCO_3$ with 5 μl of acetic anhydride at 0°C. The *N*-acetylated sCt-gp was passed through AG50X12(H^+) and dried in the presence of a tenfold molar excess of triethylamine to produce demethyl sulfoxide soluble triethylamine salts of the sCt-gp for permethylation. The resulting PMAA's were analyzed by GC-MS with a bonded OV-17 column (24 m by 0.32 mm, RSL-300, Alltech Associates) with a temperature program of 90°C (1 minute) to 200°C at 30°C per minute, held for 30 minutes. †1,3,6-tri-*O*-methyl-4-*O*-acetyl-2,5-anhydromannitol was detected in low and variable yield due to its high volatility. ‡The square brackets indicate the presence of free galactose in the α-galactosidase digest.

Features of the G-PI anchor. The biochemistry of glycosylphosphatidylinositol (G-PI)–anchored proteins has been reviewed (*18*). Of these examples, rat Thy-1 glycoprotein and *Trypanosoma brucei* variant surface glycoprotein (VSG) are the best characterized in terms of the structure of their G-PI anchors (*7*, *19*). The trypanosome is a good model system for the study of the structure and biosynthesis of G-PI anchors since the VSG coat represents about 10 percent of the total cell protein and can be readily purified in tens of milligrams.

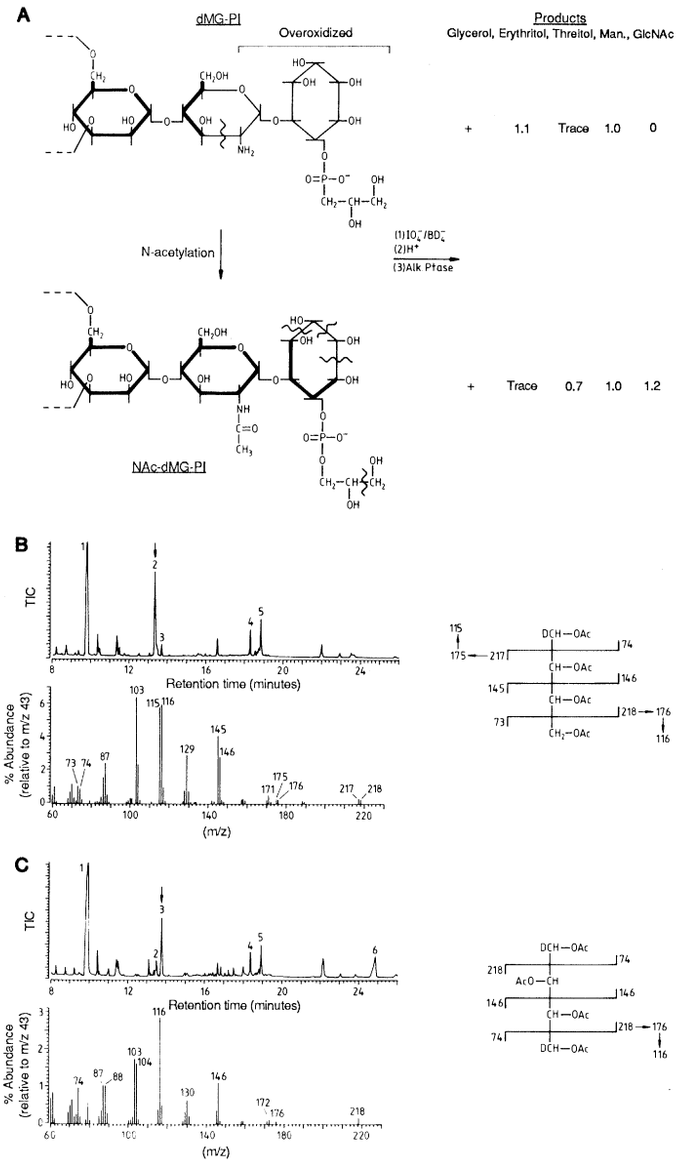

Fig. 5. Periodate oxidation of the Manα1-4GlcNH$_2$α1-6 myo-inositol core region. Samples (120 nmol) of dMG-PI and its *N*-acetylated form, NAc-dMG-PI, were periodate oxidized, and NaB^{2}H$_4$ reduced (Fig. 4). The desalted products were hydrolyzed (2*M* HCl, 100°C, 3 hours), dried, and treated with 5 units of bovine alkaline phosphatase in 15 μl of 66 m*M* NH_4HCO_3 for 24 hours at 37°C. After passage through AG50X12(H$^+$), the products were dried and per-*O*-acetylated with 15 μl of acetic anhydride and pyridine (1:1) at 100°C for 30 minutes. Samples (1 to 2 μl) were analyzed by GC-MS. The Supelcowax 10 column was used with a temperature program of 100°C (held for 2 minutes) to 260°C at 10°C per minute, held for 15 minutes. The products were quantitated from their flame ionization detector signals with the use of empirically determined relative response and hydrolytic destruction correction factors. (**A**) The periodate oxidation sites are shown by waved lines. The bold lines represent the carbon-carbon bonds resistant to oxidation. (**B**) The GC-MS analysis of the periodate-treated dMG-PI sample showing the total ion current chromatogram (upper panel) and the mass spectrum of peak 2, [1-^{2}H]erythritol (lower panel). (**C**) The GC-MS analysis of the periodate-treated NAc-dMG-PI sample showing the total ion current chromatogram (upper panel) and the mass spectrum of peak 3, [1,4-di-^{2}H]threitol (lower panel). The other numbered peaks were identified as the acetate derivatives of [1-^{2}H]glycerol, peak 1; α- and β-mannose, peaks 4 and 5; and *N*-acetylglucosamine, peak 6.

The VSG G-PI anchor as described above contains several novel structural features (Fig. 6), particularly in the glycan region. The monosaccharide sequences Galα1-2Gal, Galα1-6Gal, Galα1-3Man, Manα1-4GlcNH$_2$, and GlcNH$_2$α1-6*myo*-inositol apparently have not been previously described in eukaryotic glycoproteins.

Nonacetylated glucosamine bearing a free amino group appears to be a common feature of G-PI anchors and has been found in rat Thy-1 (*19*, *20*), human erythrocyte acetylcholinesterase (AChE) (*21*), and human erythrocyte decay accelerating factor (DAF) (*22*). Furthermore a GlcNH$_2$-inositol linkage has been inferred for *Torpedo* AChE and human placental and bovine intestinal alkaline phosphatase by deamination studies (*23*). The ethanolamine bridge between the COOH-terminal amino acid and the G-PI anchor is also conserved in Thy-1 (*19*) and human erythrocyte AChE (*21*). However, these examples (Thy-1, AChE) and DAF also contain additional ethanolamine residues with unsubstituted amino groups (*20*–*22*). Similarities in the glycan structures of several G-PI anchors are also suggested by immunological studies. A cross-reacting determinant (CRD) is present in the G-PI glycans of different sVSG's (*24*). These antibodies to CRD (anti-CRD) have also bound to PI-PLC–solubilized *Leishmania* antigen, DAF, and *Torpedo* and human erythrocyte AChE (*25*). The full extent of the structural homology indicated by anti-CRD binding must await definition of the CRD epitope. Clearly, some differences in the G-PI glycans do occur since the Thy-1 anchor contains *N*-acetylgalactosamine and no galactose (*19*). Nevertheless, it is possible that the mannose branch (Fig. 6) is conserved since the Thy-1 anchor contains comparable amounts of mannose (*19*).

A number of other glycosylated phosphoinositides exist in nature, although not linked to protein. These include the mannosylphosphatidylinositols of mycobacteria, the glycosylated inositol phosphoceramides of plants and yeasts (*26*), and a complex acidic lipophosphoglycan of *Leishmania donovani*. The last mentioned resembles a G-PI anchor in that it is a glycosyl-(lysoalkyl)-phosphatidylinositol–linked to a series of repeating disaccharide units rather than to protein (*27*). The phosphatidylinositol-glycans reported to be the precursors of second messengers for some of the actions of insulin also contain a GlcNH$_2$-inositol linkage and appear to be structurally related to G-PI anchors (*28*).

The signal for G-PI addition to nascent polypeptide resides in a short hydrophobic COOH-terminal peptide sequence which is removed and replaced by the G-PI anchor (*18*). The rapid kinetics of G-PI addition to VSG strongly suggests that the anchor is added as a unit (en bloc) to the polypeptide, and candidate precursor G-PI molecules have been identified and characterized (*29*, *30*). Whereas the G-PI biosynthetic pathway is not well understood, the composite structure (Fig. 6) indicates that it will involve several novel enzymes. However, studies on the class E thymoma mutant suggest that, for Thy-1, dolichol-phosphoryl-mannose (Dol-P-Man) may be involved in G-PI synthesis (*31*). Since enzymes that catalyze the formation of Manα1-2Man and Manα1-6Man linkages (Fig. 6) from a Dol-P-Man donor are known in the dolichol cycle of *N*-glycosylation (*32*), it is possible that G-PI biosynthesis may share one or both of these enzymes. The novel α-galactose antennae of the VSG anchor is probably added after transfer of G-PI to VSG polypeptide since the putative G-PI precursor contains only mannose (*30*). The extent and heterogeneity of galactosylation found in an individual VSG may reflect steric constraints of the attached

polypeptide to the approach of the relevant α-galactosyltransferases since there is a correlation between the degree of galactosylation with VSG subclass (*24*). These subclasses are based on COOH-terminal peptide homology where class 1 VSG's contain about 4 mol of galactose per mole of G-PI, class 2 VSG's contain eight galactose residues, and class 3 VSG's do not contain any galactose residues.

At present the functional significance of using a G-PI anchor rather than a transmembrane amino acid sequence is unknown. Possible advantages may include conservation of space in the lipid bilayer, a higher degree of lateral mobility in the bilayer, as found for Thy-1 (*33*), and the potential to be solubilized by endogenous anchor-specific phospholipases (*4*).

Note added in proof: Since submission of this article some structural details of another VSG G–PI anchor have been described (*34*).

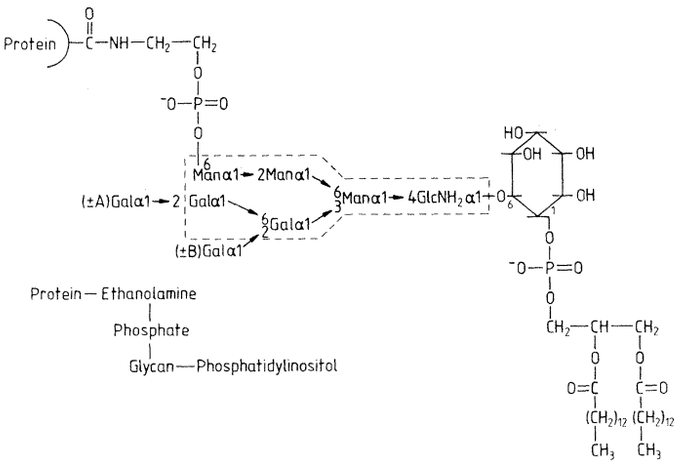

Fig. 6. Complete primary structure of the G-PI anchor of VSG variant 117. The area enclosed by the broken line represents the common region of the glycan moiety which is further substituted with one or two α1-2 linked galactose residues, residues A and B. The four structures represented account for 70 percent of all the structures present on VSG variant 117 (25 percent plus A and B, 22 percent minus A plus B, 8 percent plus A minus B, and 15 percent minus A and B).

Table 3. Exoglycosidase studies. In the left-hand column mannose residues are represented by ●, galactose by ○, and 2,5-anhydro-mannitol by ■. The glycosidic linkages are shown in the NG1 structure. The various structures were generated by exoglycosidase digestion of the whole NG fraction (NG1, -2, and -3) or individual NG substrates (NG1, NG2, or NG3). All enzyme digests were performed on NaB^3H_4-reduced glycans (Fig. 1) at substrate concentrations of 50 μ*M* in 0.1*M* sodium acetate, *p*H 5.0, for 18 hours at 37°C. The enzymes used were *Aspergillus phoenicis* Manα1-2Man specific (*16*) α-mannosidase (Apα1-2Man), 20 μg/ml; coffee bean α-galactosidase (CBα-Gal), 30 unit/ml; and jack bean α-mannosidase (JBα-Man), 60 unit/ml. The size (relative hydrodynamic volume) of each species was determined by Bio-Gel P-4 chromatography as described in Fig. 3 except that the samples were coinjected with a set of glucose oligomers (200 μg of dextran hydrolyzate). The sizes of the radioactive glycans (1 to 3 μCi) were determined by interpolation of their elution positions between the glucose oligomer elution positions as described in (*37*).

Structure	Substrate	Apα1-2Man	CBα-Gal	JBα-Man	Size (glucose units)	Structure	Substrate	Apα1-2Man	CBα-Gal	JBα-Man	Size (glucose units)
NG1	NG1	–	–	–	7.6		NG1	+	–	–	6.6
NG2	NG2	–	–	–	6.8		NG2	+	–	–	5.7
NG3	NG3	–	–	–	6.1		NG3	+	–	–	5.0
	NG1,2,3	–	+	–	4.2		NG1,2,3	–	+	+	1.7

REFERENCES AND NOTES

1. J. C. Boothroyd, *Annu. Rev. Microbiol.* **39**, 475 (1985).
2. P. Metcalf *et al.*, *Nature (London)* **325**, 84 (1987).
3. J. D. Bangs *et al.*, *Proc. Natl. Acad. Sci. U.S.A.* **82**, 3207 (1985); M. A. J. Ferguson *et al.*, *J. Biol. Chem.* **261**, 356 (1986).
4. M. L. Cardoso de Almeida and M. J. Turner, *Nature (London)* **302**, 349 (1983); R. Bulow and P. Overath, *J. Biol. Chem.* **261**, 11918 (1986); D. Hereld, J. L. Krakow, J. D. Bangs, G. W. Hart, P. T. Englund, *J. Biol. Chem.* **261**, 13813 (1986); J. A. Fox, M. Duszenko, M. A. J. Ferguson, M. G. Low, G. A. M. Cross, *J. Biol. Chem.* **261**, 15167 (1986).
5. A. A. Holder, *Biochem. J.* **209**, 261 (1983).
6. A.-M. Strang *et al.*, *ibid.* **234**, 481 (1986).
7. M. A. J. Ferguson *et al.*, *J. Biol. Chem.* **260**, 14547 (1985); B. Schmitz *et al.*, *Mol. Biochem. Parasitol.* **20**, 191 (1986).
8. G. A. M. Cross, *J. Cell. Biochem.* **24**, 79 (1984).
9. M. A. J. Ferguson and G. A. M. Cross, *J. Biol. Chem.* **259**, 3011 (1984).
10. M. W. Clarke, R. W. Olafson, T. W. Pearson, *Mol. Biochem. Parasitol.* **17**, 19 (1985).
11. M. A. J. Ferguson, K. Haldar, G. A. M. Cross, *J. Biol. Chem.* **260**, 4963 (1985).
12. The Pronase digest (2 ml) was acidified with 20 μl of acetic acid, 0.5 ml of 2-propanol was added, and the mixture was centrifuged. The supernatant was applied to a 5-μm Ro-Sil C8 column (0.46 by 25 cm, Alltech Associates) in sequential 0.5-ml injections and eluted with a gradient of 20 to 100 percent 2-propanol in 0.05 percent aqueous trifluoroacetic acid over 80 minutes at 0.8 ml/min. The G-PI moiety was detected by following a [^{3}H]myristic acid label and was eluted between 53 and 77 percent 2-propanol. The G-PI fractions were dried by rotary evaporation at 25°C and stored in 56 percent 2-propanol at −20°C.
13. J. H. Duncan, W. J. Lennarz, C. C. Fenselau, *Biochemistry* **10**, 927 (1971).
14. dMG-PI (120 nmol) was *N*-acetylated in 100 μl of saturated $NaHCO_3$ by three additions of 2.5 μl of acetic anhydride 10 minutes apart. The product was desalted by passage through AG50X12(H^+) and evaporation with toluene.
15. Permethylated glycans were purified on a 5-μm Ro-Sil C18 column (0.46 by 25 cm, Alltech Associates) eluted with a gradient of acetonitrile in H_2O, 25 to 65 percent, over 60 minutes at 1 ml/min. Permethylated NG1, NG2, and NG3 fractions eluted at 49, 46, and 42 percent acetonitrile, respectively.
16. A. Kobata, in *Biology of Carbohydrates*, V. Ginsberg and P. W. Robbins, Eds. (Wiley, New York, 1984), vol 2, pp. 87–162.
17. R. W. Jeanloz and E. Forchielli, *J. Biol. Chem.* **188**, 361 (1951).
18. G. A. M. Cross, *Cell* **48**, 179 (1987); M. G. Low, *Biochem. J.* **244**, 1 (1987).
19. A. G. D. Tse *et al.*, *Science* **230**, 1003 (1985); A. F. Williams and A. G. D. Tse, *Biosci. Rep.* **5**, 999 (1985).
20. S. H. Fatemi *et al.*, *J. Biol. Chem.* **262**, 4728 (1987).
21. R. Hass, P. T. Brandt, J. Knight, T. L. Rosenberry, *Biochemistry* **25**, 3098 (1986).
22. M. E. Medof, E. I. Walter, W. L. Roberts, R. Haas, T. L. Rosenberry, *ibid.*, p. 25.
23. M. G. Low *et al.*, *Biochem. J.* **241**, 615 (1987).
24. A. A. Holder, *Curr. Top. Microbiol. Immunol.* **117**, 57 (1985).
25. C. Bordier, R. J. Etges, J. Ward, M. J. Turner, M. L. Cardoso de Almeida, *Proc. Natl. Acad. Sci. U.S.A.* **83**, 5988 (1986); M. A. Davitz, A. M. Gurnett, M. G. Low, M. J. Turner, V. Nussenzweig, *J. Immunol.* **138**, 520 (1987); A. Steiger, M. L. Cardoso de Almeida, M. C. Blatter, U. Brodbeck, C. Bordier, *FEBS Lett.* **199**, 182 (1986).
26. H. E. Carter, D. R. Strobach, J. N. Hawthorne, *Biochemistry* **8**, 383 (1969); Y. C. Lee and C. E. Ballou, *ibid.* **4**, 1395 (1965); T. C. Y. Hsieh, K. Kaul, R. A. Laine, R. L. Lester, *ibid.*, **17**, 3575 (1978).
27. S. J. Turco *et al.*, *ibid.* **26**, 6233 (1987).
28. A. R. Saltiel, J. A. Fox, P. Sherline, P. Cuatrecasas, *Science* **233**, 967 (1986).
29. J. L. Krakow *et al.*, *J. Biol. Chem.* **261**, 12147 (1986).
30. A. K. Menon *et al.*, *ibid.*, in press.
31. S. H. Fatemi and A. M. Tartakoff, *Cell* **46**, 653 (1986); A. Conzelmann, A. Spiazzi, R. Hyman, C. Bron, *EMBO J.* **5**, 3291 (1986).
32. C. B. Hirschberg and M. D. Snider, *Annu. Rev. Biochem.* **56**, 63 (1987).
33. A. Ishihara, Y. Hou, K. Jacobson, *Proc. Natl. Acad. Sci. U.S.A.* **84**, 1290 (1987).
34. B. Schmitz *et al.*, *Biochem. Biophys. Res. Commun.* **146**, 1055 (1987).
35. I. Ciucanu and F. Kerek, *Carbohydr. Res.* **131**, 209 (1984).
36. D. P. Sweet, R. H. Shapiro, P. Albersheim, *ibid.* **40**, 217 (1975).
37. R. B. Parekh *et al.*, *Nature (London)* **316**, 452 (1985).
38. S. W. Homans *et al.*, *Biochemistry* **25**, 6342 (1986).
39. A. De Bruyn, M. Anteunis, G. Verhegge, *Acta Ciencia Ind.* **1**, 83 (1975).
40. W. R. Sherman *et al.*, *Anal. Biochem.* **78**, 119 (1977).

41. Supported in part by a grant from the Wellcome Trust. The Oxford Oligosaccharide Group is supported by Monsanto Company. We thank J. A. Fox and G. A. M. Cross for sVSG; D. A. Ashford, S. E. Zamze, and R. B. Parekh for advice; K. Haldar, M. G. Low, I. Silman, A. F. Williams, and T. L. Rosenberry for helpful discussions; and F. Homans for typing the manuscript.

22 June 1987; accepted 14 December 1987